How Long Can The Escaping Ant Be Confined?

Kossi Roland Etse
DAVID Lab., UVSQ, Université Paris Saclay, 45 avenue des Etats-Unis, 78000, Versailles, France

Abstract

Langton's ant is a simple two-dimensional cellular automaton whose long-term behavior exhibits remarkable complexity. While it is known that the ant eventually escapes any finite connected region of the grid, the quantitative aspects of this escape remain poorly understood. In this paper, we study the *escaping time* of Langton's ant, defined as the maximum number of steps the ant can perform within a finite connected domain before leaving it.

We establish general upper bounds on the escaping time as a function of the domain size, and derive improved bounds for rectangular domains. In particular, we obtain a factorial upper bound for square domains via an inductive decomposition argument. We also obtain linear upper bounds for rectangular domains of height two and three via a column-by-column analysis. More generally, for rectangular domains with a fixed height, we establish a polynomial upper bound in the number of columns. These results are complemented by exact values computed through an optimized simulation algorithm that exploits the geometric symmetries of the grid and employs a backtracking branching strategy to avoid exhaustive search over all color configurations. We also provide lower-bound constructions, proving that the linear upper bounds for rectangular domains of heights two and three are asymptotically optimal.

2012 ACM Subject Classification Mathematics of computing

Keywords and phrases Langton's Ant, Escaping Time, Finite Grid Dynamics, Combinatorial Bounds, Discrete Dynamical Systems, Cellular Automata

Digital Object Identifier 10.4230/LIPIcs.MFCS.2026.49

Related Version *Full Version*: `https://arxiv.org/abs/2606.26677`

Supplementary Material *InteractiveResource*: `https://ekroland.github.io/TEA/`

Acknowledgements I would like to thank David Auger and Pierre Coucheney for valuable discussions and insightful feedback. I also thank Jérémie Cabessa and Yann Strozecki for their help with the simulations, and anonymous reviewers for their comments and suggestions.

1 Introduction

Many natural and artificial systems can be modeled as collections of simple interacting elements evolving over discrete time. Each element updates its state according to local rules that depend only on a small neighborhood, yet the repeated application of these rules can generate complex global behavior. Understanding how such macroscopic patterns arise from microscopic interactions, often referred to as *emergence*, is a central question in the study of discrete dynamical systems.

A classical example of emergence in a discrete dynamical system is *Langton's ant*, a two-dimensional cellular automaton introduced by Christopher G. Langton in 1986 in the context of artificial life [10]. Langton's ant is defined on the infinite square grid whose cells are in one of two states: *black* (turn-left) or *white* (turn-right). The ant occupies a cell and has an orientation among the four cardinal directions. At each step, the ant turns left on a black cell and right on a white cell, flips the state of the cell, and moves forward to the adjacent cell in the new direction.

Despite the simplicity of these local rules, the trajectory of the ant exhibits highly unpredictable behavior. Starting from a uniformly white (or black) initial configuration, the ant's trajectory shows rotational symmetry during the first 500 steps, followed by an

51st International Symposium on Mathematical Foundations of Computer Science (MFCS 2026).
Editors: Michal Koucký and Daniela Petrişan; Article No. 49; pp. 49:1–49:17
Leibniz International Proceedings in Informatics
LIPICS Schloss Dagstuhl – Leibniz-Zentrum für Informatik, Dagstuhl Publishing, Germany

apparently erratic phase lasting until around step 10 000, after which the trajectory suddenly becomes regular: the ant advances indefinitely along one of the four diagonal directions, tracing a periodic pattern of period 104 known as the *highway* (Figure 1). Numerical simulations consistently show that this highway emerges from any finite initial configuration (configuration in which all but a finite number of cells are in the same state), yet this experimental observation has never been formally established.

Beyond the standard two-dimensional square lattice, Langton's ant has been studied on a variety of other regular structures and topologies, including one-dimensional lattices [3, 8], triangular and hexagonal grids [8, 13], infinite bi-regular and hyperbolic graphs, finite and planar graphs [4], twisted tori [9], and higher-dimensional lattices [1]. Those works show that the dynamical behavior of the ant is strongly influenced by the topology of the underlying graph. Generalizations have also been proposed along other axes: variants with a richer set of movements and multi-state extensions [5, 7].

While much attention has been devoted to the ant's behavior on infinite grids, its dynamics on finite domains remain poorly understood. It is known that Langton's ant eventually escapes any finite connected region of the grid, yet the quantitative aspects of this escape – and more broadly, the computational complexity of predicting its behavior on finite two-color grids – are still unclear. A natural and fundamental question thus arises: *how long can the ant remain confined within a finite region before escaping?* Bounding the escaping time provides insight into the complexity of reachability problems and prediction difficulty for the ant on finite domains.

The Present Work

This paper studies the escaping time of Langton's ant on the standard two-color square grid from a quantitative perspective, without modifying the cell states or the underlying topology. Our contributions are as follows.

We first establish that, while confined to a finite connected domain, the same color configuration cannot appear twice in the ant's trajectory. This immediately yields a general upper bound of 2^d on the escaping time for any domain of d cells.

We then derive improved bounds depending on the shape of the domain. For square domains with n rows and n columns, an inductive decomposition into a boundary layer and interior yields a factorial upper bound $(n+1)!$. For rectangular domains of height two, a column-by-column analysis gives the linear bound $6(n-1)$ for a grid with n columns, which is tight: we exhibit explicit configurations achieving exactly $6(n-1)$ steps. For rectangular domains of height three, the same approach yields the linear bound $10n-4$, with near-matching constructions. More generally, for fixed k, an inductive argument gives for rectangular domains with k rows and n columns an upper bound $\left(\frac{n+1}{\sqrt{2}}\right)^k$, which is polynomial in n for every fixed k.

These results are complemented by exact escaping times computed for all rectangular grids up to size 9×9, using an optimized simulation algorithm that exploits grid symmetries and a backtracking branching strategy, which in particular corrects and extends the OEIS sequence A282425 [11].

The remainder of this paper is organized as follows. Section 2 introduces the formal framework, definitions, and known results. Section 3 presents our general results on finite connected domains, including the proof that color configurations cannot repeat. Section 4 details our simulations (4.1), the inductive derivation of the square domain bound (4.2), the linear bounds for two-row (4.3.1) and three-row (4.3.2) rectangular grids and the inductive derivation of the bound of rectangular domain with fixed height (4.4).

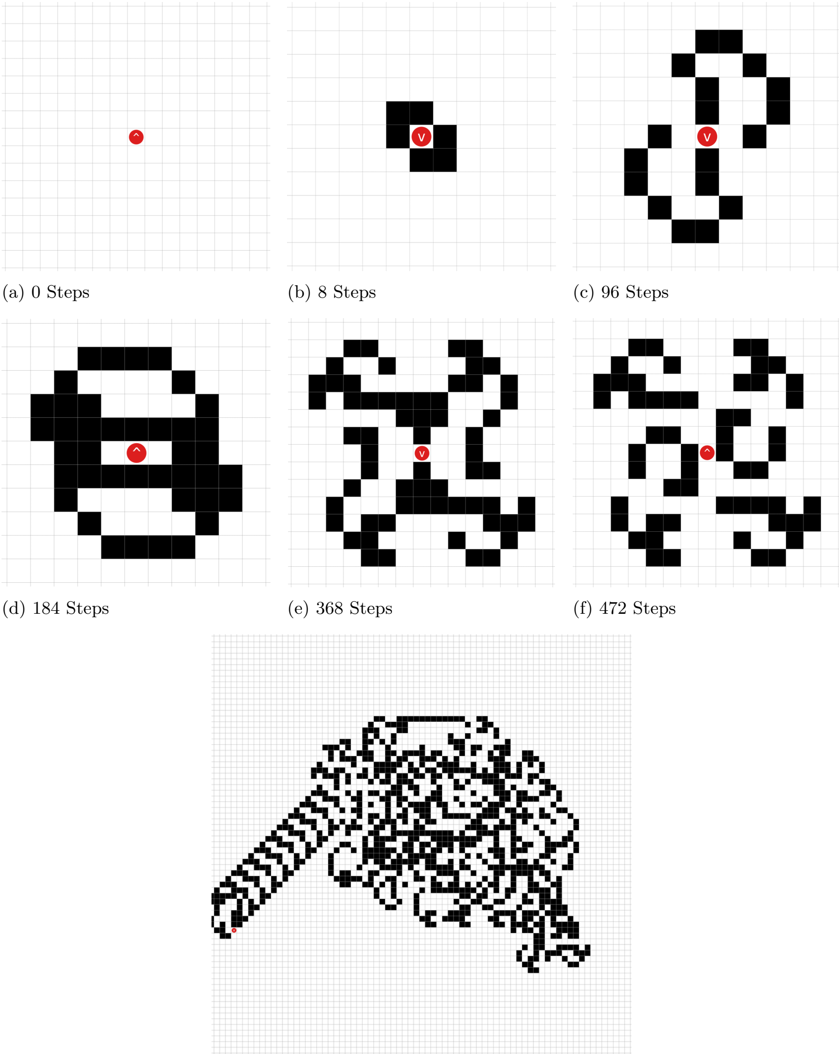

(a) 0 Steps (b) 8 Steps (c) 96 Steps

(d) 184 Steps (e) 368 Steps (f) 472 Steps

(g) Highway

Figure 1 The ant starting from a uniform white configuration facing north. Snapshots (a–f) after steps 8, 96, 184, 368, and 472 illustrate the early rotational symmetry, while (g) shows the eventual *highway* regime.

2 Preliminaries

This section introduces the concepts, definitions, and notation that will be used throughout the paper.

2.1 Graph Representation and Transition Function

We represent the infinite grid as a planar directed graph $G = (V, A)$, where the vertex set $V = \mathbb{Z}^2$ corresponds to the cells, and A consists of arcs in both directions between vertices corresponding to adjacent cells (i.e. pairs of vertices differing by exactly one unit in exactly one coordinate). See Figure 2 for an illustration, where each pair of opposite arcs is represented as single undirected edge. In this representation, the position of the ant (the cell it occupies and its orientation) is encoded by an arc $(u, v) \in A$, specifying both the cell u

from which the ant arrives and the cell v toward which it is heading. We identify vertices with cells of the grid and arcs with oriented positions of the ant. Thus, we may use "cell" for vertices and "position" for arcs.

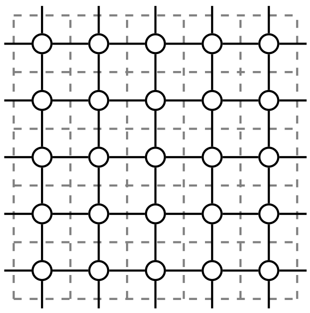

Figure 2 Representation of a portion of the infinite grid as a planar directed graph $G = (V, A)$: vertices correspond to cells, and each undirected edge represents a pair of arcs in both directions between adjacent cells.

In all figures cited in the remainder of this paper, black cells are in the L state and white cells in the R state. Gray cells represent cells whose state may be either L or R and is not yet fixed.

A *color configuration* of the grid is a function $C : \mathbb{Z}^2 \to \{L, R\}$ assigning to each cell its state, where L denotes the turn-left state and R denotes the turn-right state. A *configuration* is a pair (C, pos) consisting of a color configuration of the grid together with the position $pos \in A$ currently occupied by the ant.

The global *transition function* T is defined by $T(C, pos) = (C', pos')$, where, given $pos = (u, v)$:

- $C'(w) = C(w)$ for all $w \neq v$, and $C'(v) = \overline{C(v)}$, where $\overline{L} = R$ and $\overline{R} = L$;
- $pos' = (v, w)$, where w is the neighbor of v obtained by turning right from the direction $(u \to v)$ if $C(v) = R$, or turning left if $C(v) = L$.

Applying T once corresponds to executing one step of the ant's motion. See Figure 3 for an illustration of the application of transition function.

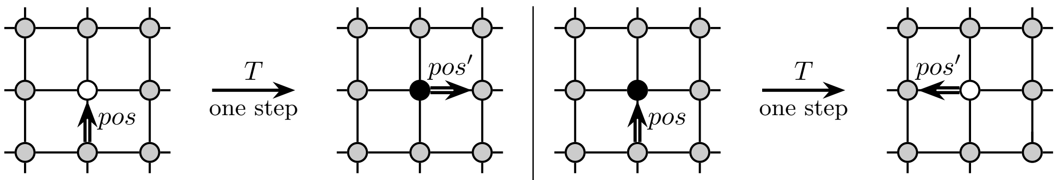

(a) Right turn. **(b)** Left turn.

Figure 3 Configuration before and after one application of the transition function T. In (a), the ant arrives at a white cell, turns right, flips the cell to black, and moves forward. In (b), the ant arrives at a black cell, turns left, flips the cell to white, and moves forward.

▶ Remark 1. An important property is that the dynamics of the ant is deterministic and *reversible*, i.e. the transition function is bijective. Configurations at each time in the future and in the past are entirely determined by the current configuration. To determine the previous configuration, it is enough to invert the direction of the ant, to apply the transition function T, and to invert once more the direction of the ant.

2.2 HV-partition Property

Another fundamental structural property of Langton's ant is what we call the *HV-partition property*. The ant's orientation alternates between horizontal and vertical, since its direction is rotated by a quarter turn at each step. Color the cells of G in a checkerboard pattern by assigning one color to all cells (i, j) with $i + j$ even, and the other color to those with $i + j$ odd. If the ant starts in a horizontal orientation and is pointing toward a cell of the first color, then it will always be in a horizontal orientation when pointing toward a cell of that color, and in a vertical orientation when pointing toward a cell of the other color. This induces a natural partition of $\mathbb{Z}^2$ into two classes, *H-cells* and *V-cells*: when the ant points toward an H-cell (resp. a V-cell), it arrives horizontally (resp. vertically) and departs vertically (resp. horizontally). See Figure 4 for illustration.

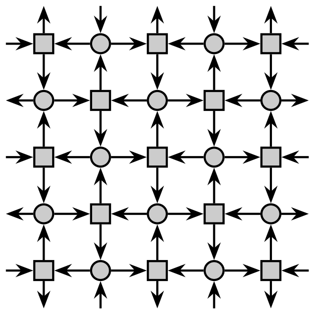

Figure 4 Illustration of the HV-partition property under the assumption that the ant enters horizontally into the cell located in the last row of the first column. V-cells are represented as circles and H-cells as rectangles. Horizontal arcs point toward H-cells, and vertical arcs point toward V-cells. The set of arcs thus specifies exactly all admissible positions of the ant.

This partition of the cells induces a corresponding partition of the arc set A into two subsets A_H and A_V, where A_H (resp. A_V) is the set of admissible positions of the ant when the origin cell $(0, 0)$ is taken as an H-cell (resp. a V-cell). So according to the starting position of the ant the motion of the ant will be either supported by the graph $(\mathbb{Z}^2, A_H)$ (horizontal G) or $(\mathbb{Z}^2, A_V)$ (vertical G). In these graphs, every cell has exactly two incoming arcs and exactly two outgoing arcs.

2.3 Finite Connected Domain

We say that a finite set of cells $V_D \subset \mathbb{Z}^2$ is *connected* if for any two cells $u, v \in V_D$, there exists a sequence $u = v_0, v_1, \ldots, v_k = v$ in V_D with $k \in \mathbb{N}$ such that v_{i+1} is adjacent to v_i for every $0 \leq i \leq k - 1$.

For any such set, we define the associated *finite connected domain* $D = (V_D, A_D)$, where A_D consists of all arcs of A incident to at least one cell of V_D. Three types of arcs in A_D can be distinguished: *interior arcs*: both endpoints in V_D; *in-boundary arcs*: tail outside V_D, head in V_D and *out-boundary arcs*: tail in V_D, head outside V_D.

The HV-partition of G restricts naturally to D: the arc set A_D is partitioned into $A_D \cap A_H$ and $A_D \cap A_V$, identifying within D the admissible positions of the ant under each of the two partitions. We define *horizontal* D as $(V_D, A_D \cap A_H)$ and *vertical* D as $(V_D, A_D \cap A_V)$. Henceforth, unless stated otherwise, D refers to horizontal D (i.e $A_D = A_D \cap A_H$).

A cell of D is called a *boundary cell* if it is incident to at least one boundary arc (either an in-boundary or an out-boundary arc), and a *corner cell* if it is incident to both an in-boundary and an out-boundary arc. See Figure 5 for an illustration.

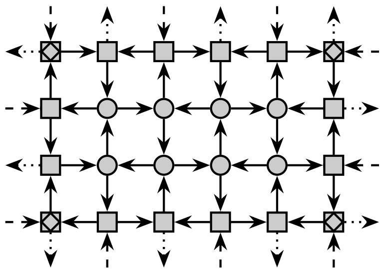

Figure 5 A horizontal finite connected domain of four rows and six columns. Interior cells are shown as circles, boundary cells as rectangles, and corner cells as diamonds; interior arcs are drawn as solid lines, in-boundary arcs as dashed lines and out-boundary arcs as dotted lines. Arc directions are determined by HV-partition.

A color configuration of D is a function $C_D : V_D \to \{L, R\}$, and a configuration of D is a pair (C_D, pos), where $pos \in A_D$. The ant is said to be *confined* in D as long as its position is an interior or in-boundary arc of D, and it *escapes* D at the first step at which its position is an out-boundary arc of D. The transition function T restricts naturally to D.

Given an initial configuration (C_0, pos_0) of D with $pos_0 = (v_0, v_1)$, for $k \in \mathbb{N}$, we denote by $(C_k, pos_k) = T^k(C_0, pos_0)$ with $pos_k = (v_k, v_{k+1})$, the configuration after k steps. The *trajectory* of the ant from (C_0, pos_0) to (C_k, pos_k) is the sequence of configurations $(C_i, pos_i)_{0\leq i\leq k}$. The *set of exited cells* during this trajectory is the set $\{v_i \mid 1 \leq i \leq k\}$ consisting of all cells that the ant leaves during its motion. The positions pos_0 and pos_k are the starting and ending positions of the trajectory, respectively, and v_1 and v_k are called the starting and ending cells.

The *motion of the ant within* D from (C_0, pos_0) refers to any trajectory $(C_i, pos_i)_{0\leq i\leq k}$ such that each pos_i is an arc of D.

The *number of steps performed* by the ant within D starting from (C_0, pos_0) is:

$$S_D(C_0, pos_0) = \min \{k \in \mathbb{N} \mid v_{k+1} \notin V_D\},$$

the number of steps during which it remains confined in D. The *escaping time* of D is defined as:

$$S_D = \max \{S_D(C_0, pos_0) \mid (C_0, pos_0) \text{ configuration of } D\},$$

that is, the maximum number of steps the ant can perform within D over all initial configurations. The central question addressed in this paper is the following:

Escaping Time Problem. *Given a finite connected domain D of the grid, what is the escaping time of D?*

2.4 Related Work

The most fundamental result on Langton's ant on the infinite square grid, due to Troubetzkoy [12], states that for any initial configuration, if the ant moves indefinitely, the set of cells exited infinitely often contains no corner cell. As a corollary [2], the ant's trajectory is always *unbounded* (non-periodic). Consequently, the ant escapes any finite connected domain in a finite number of steps. The main objective of this paper is to quantify this escaping time.

The other main theoretical results concern the computational complexity of the ant. Gajardo, Moreira, and Goles [6] showed that Boolean circuits can be simulated within Langton's ant by embedding logic gadgets into the initial color configuration of the grid, with the ant's trajectory serving as the computational signal. This yields the P-hardness under log-space reductions of the reachability problem: given an initial configuration, does the ant ever visit a specified target cell? By further composing these gadgets to simulate one-dimensional cellular automata, they established that Langton's ant is computationally universal, which in turn implies the existence of undecidable problems about its trajectory.

When the ant is restricted to a finite domain, this reachability problem becomes decidable. But what is its precise complexity? In particular, is it P-complete? If the escaping time was polynomially bounded, then reachability on finite grids can be decided by direct simulation in polynomial time, suggesting that the problem lies strictly within P.

Tsukiji and Hagiwara established PSPACE-hardness results concerning the predictability and macroscopic behavior of the ant. On the square grid [13], by introducing a third cell state in which the ant moves straight ahead without changing the cell's color, they proved that determining whether a given finite configuration is repeatable (i.e. the ant's trajectory is bounded and eventually cycles through a finite sequence of configurations) is PSPACE-complete. They also established the PSPACE-hardness of this problem on a hexagonal grid. These results are obtained through a reduction from the Quantified Boolean Formula (QBF) evaluation problem. In a subsequent study on a twisted torus [9], they proved that it is PSPACE-hard to determine whether the ant will ever visit almost all vertices or nearly none of them via a reduction from the Quantified Conjunctive Normal Form (QCNF) problem. The introduction of the third state on the square grid and the use of the twisted torus topology are crucial for these reductions. These break the standard HV-partition of the square grid and allows the ant to be "reversed", so that it can traverse arcs in both directions. This property is exploited in the reductions through the reversible behavior of the system.

On the standard two-color square grid, however, the HV-partition is a rigid structural constraint: the ant cannot be reversed, and every arc is traversed in a fixed direction. This raises the question of whether PSPACE-hardness can be achieved without breaking the HV-partition, or whether every natural decision problem about the ant on the finite two-color square grid is solvable in polynomial time. Quantifying the escaping time is a necessary first step toward answering this question.

3 Escaping Time of Finite Connected Domains

Let D be a finite connected domain of $d \in \mathbb{N}^*$ cells. Since each cell can be in one of two states, there are 2^d color configurations of D. By the HV-partition, each cell is the head of exactly two arcs in A_D, giving $2d$ admissible positions. Together with 2^d possible color configurations, the total number of configurations of D is $2d \cdot 2^d$. The unboundedness result ensures that the ant's trajectory cannot be periodic within D, so no configuration of D can be encountered twice in the trajectory of the ant within D, and the escaping time of D is bounded by $2d \cdot 2^d$. However, this bound is far from tight, and the following results provide a slight improvement.

▶ **Proposition 2.** *Starting from a configuration of a finite connected domain D, no color configuration of D can appear twice in the motion of the ant within D.*

Sketch of the Proof. Suppose, for contradiction, that some color configuration C_D appears twice during the ant's motion within D. Let $Traj$ denote the trajectory of the ant between the first and second occurrences of C_D. Since the successive positions of the ant during its trajectory form a connected path, the set of exited cells during $Traj$ induces a finite connected subdomain of D, which we denote by D'. As the configuration C_D is identical at the beginning and end of $Traj$, the state of each cell in D' must be flipped an even number of times during $Traj$. Consequently, the ant must exit each cell of D' a positive even number of times. The contradiction follows from the two claims below.

▷ Claim 1. Every corner cell of D' is either a starting cell or an ending cell of $Traj$.

▷ Claim 2. D' has at least three distinct corner cells.

Claims 1 and 2 together imply that the trajectory $Traj$ has at least two distinct starting cells or at least two distinct ending cells, contradicting the fact that each ant trajectory has a unique starting and a unique ending cell. Thus, no coloring of D can appear twice during the ant motion within D. ◀

▶ **Corollary 3.** *For any finite connected domain D of $d \in \mathbb{N}^*$ cells, one has $S_D \leq 2^d$.*

This bound is, however, also far from being achieved in practice. In the following sections, we present simulation results on the escaping time over rectangular domains, which suggest that the true maximum grows significantly slower than 2^d, and we establish rigorous upper bounds for square connected domains and some rectangular connected domains.

We end this section by pointing out that:

▶ Remark 4. In order to maximize the number of steps performed within a finite connected domain D, the ant must start from an in-boundary arc of D.

Indeed, if the maximal number of steps were achieved by an ant starting from an interior arc, then, by reversibility of the transition function, this number could be extended, contradicting maximality.

4 Escaping Time of Square and Rectangular Connected Domains

We now focus on rectangular finite connected domains. For $k, n \in \mathbb{N}^*$, we denote by $G_{k,n}$ the rectangular domain with k rows and n columns. The *horizontal* $G_{k,n}$ is the graph equipped with the HV-partition in which the cell in the last row of the first column is an H-cell; the alternative partition is referred to as the *vertical* $G_{k,n}$. We denote by $S_{k,n}$ the maximum escaping time over both horizontal $G_{k,n}$ and vertical $G_{k,n}$.

The goal of this section is twofold: we first present exact values of $S_{k,n}$ obtained by computer simulation, which serve both as a reference and as a guide for the theoretical bounds established thereafter; we then prove rigorous bounds for square connected domains and some rectangular connected domains.

4.1 Exact Escape Times via Simulation on Small Grids

We computed the exact values of $S_{k,n}$ for $1 \leq k, n \leq 9$ (Table 1). The values $S_{n,n} - 1$ up to $n = 7$ were previously listed as sequence A282425 in the OEIS [11], with an error of 1 for $S_{7,7}$; our values correct this entry.

An interactive simulator of Langton's ant is available at `https://ekroland.github.io/TEA/`, together with the configurations achieving these escape times. The simulator allows users to replay the ant's trajectory step by step from each of these configurations.

Table 1 Values of $S_{k,n}$ for $1 \le k, n \le 9$.

	1	2	3	4	5	6	7	8	9
1	1	2	2	2	2	2	2	2	2
2		6	12	18	24	30	36	42	48
3			17	28	37	48	57	68	77
4				46	64	86	104	146	156
5					85	130	145	214	221
6						164	220	280	315
7							262	356	410
8								488	618
9									679

4.2 Upper Bound of the Escaping Time of Square Domains

In this section, we consider the square finite connected domain $G_n = G_{n,n}$ with $n \in \mathbb{N}^*$ and investigate the growth of $S_n = S_{n,n}$. Note that G_n has $2n^2 \cdot 2^{n^2}$ configurations and by Corollary 3, $S_n \le 2^{n^2}$. In this section, we derive an improved upper bound using an inductive approach, expressing S_n in terms of S_{n-2}.

▶ **Theorem 5.** *For each positive integer n, we have $S_n \le (n+1)!$.*

Proof. By simulation: $S_1 = 1$ and $(1+1)! = 2$, $S_2 = 6$ and $(2+1)! = 6$ thus the inequality is true for $n \in \{1, 2\}$.

For $n \ge 3$, observe that G_n can be decomposed as the union of G_{n-2} and B_n, where B_n denotes the connected domain on the boundary cells of G_n (see Figure 6). This decomposition provides the basis for our inductive argument.

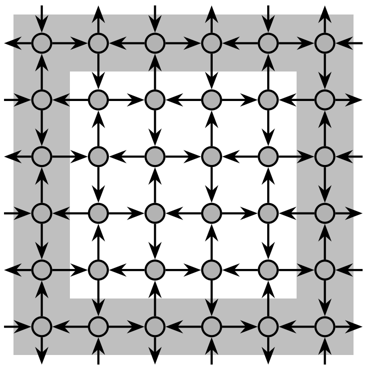

Figure 6 Decomposition of G_6 as the union of boundary cells B_6 (gray shaded region) and interior grid G_4 (white region).

To maximize the number of steps on G_n, the ant must start at an in-boundary arc of G_n (Remark 4). From this starting position, it reaches an in-boundary arc of G_{n-2} within at most two or three steps when a corner cell is involved. Then it performs some number of steps within G_{n-2} before reaching an out-boundary arc of G_{n-2} thereby returning to B_n. Once in B_n, the ant undergoes a bouncing phase before re-entering G_{n-2}. Each such bouncing phase requires at most two steps or three steps when a corner cell is involved. The process then repeats: the ant alternates between phases inside G_{n-2} and bouncing phases within

B_n until it finally exits G_{n-2} for the last time and reaches an out-boundary arc of G_n in at most three additional steps. Suppose that the ant returns to G_{n-2} at most X_n times after its initial entry, then we obtain:

$$S_n \leq 3 + (X_n + 1) \cdot S_{n-2} + 3X_n + 3,$$

where the four terms account, respectively, for: the initial steps to enter G_{n-2} from an in-boundary arc of G_n; the $(X_n + 1)$ visits to G_{n-2} (initial entry plus X_n returns); the X_n bouncing phases on B_n; and the final steps to escape G_{n-2} to an out-boundary arc of G_n. This simplifies to:

$$S_n \leq (X_n + 1) \cdot S_{n-2} + 3X_n + 6.$$

It remains to bound X_n. To this end, we analyze the behavior of the ant on the top row of B_n and determine the maximal number of times it can bounce there while still being able to return to G_{n-2}. During a bouncing phase, the ant moves from G_{n-2}, traverses boundary cells, and returns to G_{n-2}, without occupying any in-boundary or out-boundary arc of G_n.

For example, Figure 7 illustrates all possible bounces in the top row of B_{10} along with the maximum number of times each can be performed.

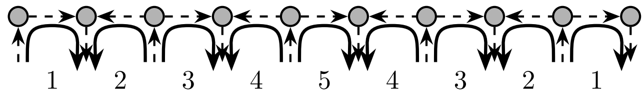

Figure 7 Top row of B_{10} with curved solid lines indicating possible bouncing motions and the corresponding maximal number of times each bounce can occur.

Each of the two corner cells of the top row can be used to perform only one type of bounce, which can occur at most once. Indeed, after a corner cell is used for a bounce, its color is updated, and the ant's next visit to that cell immediately leads to an out-boundary arc of G_n in a single step.

In general, each non-corner cell in the top row can be used to perform two types of bouncing motions - left and right - depending on which side of the cell is located the horizontal arc that is involved in the bounce. Moreover, for each such cell, the counts of left and right bounces can differ by at most one, since consecutive visits to a given cell must alternate between the two directions due to the color-alternation property.

Combining these two observations, the number of possible bounces on the top row of B_n is bounded by:

$$\begin{cases} 1 + 2 + ... + (\frac{n}{2} - 1) + \frac{n}{2} + (\frac{n}{2} - 1) + ... + 2 + 1 = \frac{n^2}{4} & \text{if n is even} \\ 1 + 2 + ... + (\frac{n-1}{2} - 1) + \frac{n-1}{2} + \frac{n-1}{2} + (\frac{n-1}{2} - 1) + ... + 2 + 1 = \frac{n^2-1}{4} & \text{if n is odd} \end{cases}$$

By symmetry across the four sides of B_n, we obtain $X_n \leq 4 \cdot \frac{n^2}{4} = n^2$. Substituting in $S_n \leq (X_n + 1) \cdot S_{n-2} + 3X_n + 6$, we obtain: $S_n \leq \left(n^2 + 1\right) S_{n-2} + 3n^2 + 6$. From this inequality, using some technical arguments, it can be deduced that $S_n \leq (n + 1)!$. ◀

4.3 Linear bound of the Escaping Time of Some Rectangular Domains

In this section, we focus on the escaping time of rectangular finite connected domains consisting of two or three rows and an arbitrary number of columns. Our approach to determining the escape time of these domains consists in bounding the number of steps the ant can perform within each column of the domain before the termination of its motion within the entire domain. These columns – horizontal or vertical $G_{2,1}$ or $G_{3,1}$ – can be interpreted as gadgets consisting of entry arcs (the in-boundary arcs), exit arcs (the out-boundary arcs), and an internal state determined by the color configuration. Given its internal state and the specific entry arc through which the ant enters, the gadget updates its internal state and directs the ant toward one of its exit arcs. There are four possible types of motion that the ant can perform on every such column:

- *Bouncing*: the ant enters and leaves through the same side of the column;
- *Crossing*: the ant enters through one side of the column and exits through the opposite side;
- *Initial*: the ant enters the grid through an in-boundary arc at the top or bottom of the column;
- *Out*: the ant exits the grid through an out-boundary arc at the top or bottom of the column.

Initial and out motions are performed in one step, bouncing and crossing motions in two steps.

4.3.1 Two-row Grids

When viewed column by column, a two-row grid (either vertical or horizontal) can be seen as an alternating succession of horizontal and vertical $G_{2,1}$ (See Figure 8).

Since horizontal and vertical $G_{2,1}$ are symmetric by a half turn rotation, it suffices to restrict our analysis to the horizontal $G_{2,1}$; all results extend to vertical $G_{2,1}$ by symmetry.

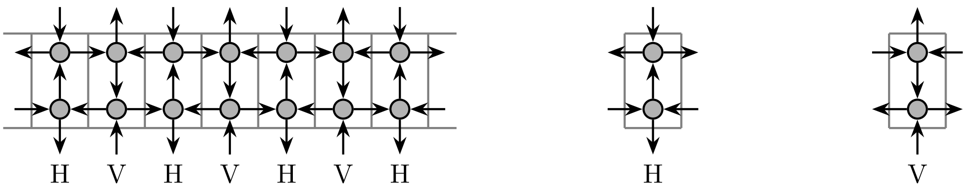

(a) Portion of two-row grid. **(b)** Horizontal $G_{2,1}$. **(c)** Vertical $G_{2,1}$.

Figure 8 Two-row grid viewed by columns.

The following result analyzes, for each type of motion performed by the ant upon its first visit to a horizontal $G_{2,1}$, the maximum number of steps it can perform within this horizontal $G_{2,1}$ during its motion within the entire two-row grid. This is done by counting the steps of the initial motion together with those of any subsequent motions upon return.

▶ **Lemma 6.** *During its motion within a two-row grid, if the motion performed by the ant upon its first visit to a column that is a horizontal $G_{2,1}$ is:*

1. *an out motion, then the ant performs at most one step within this column before escaping the two-row grid;*
2. *a bouncing motion, then the ant performs at most three steps within this column before escaping the two-row grid. Moreover, these three steps consist of the bouncing motion and an out motion;*
3. *an initial motion, then the ant performs at most four steps within this column before escaping the two-row grid. Moreover, these four steps consist of the initial motion, a bouncing motion and an out motion;*
4. *a crossing motion, then the ant performs at most six steps within this column before escaping the two-row grid. Moreover, these six steps consist of three crossing motions, two of which occur in the same direction.*

Using Lemma 6, we can now bound the total escaping time of a two-row grid. The grid $G_{2,n}$ has two boundary columns and $n-2$ interior columns. To maximize the number of steps, the ant must perform a crossing motion on each interior column upon its first visit and a bouncing or initial motion within each boundary column. This yields $S_{2,n} \leq 6(n-2)+6 = 6(n-1)$.

▶ **Theorem 7.** *For every integer $n \geq 2$, one has $S_{2,n} \leq 6(n-1)$.*

This bound is tight. Figure 9 exhibits explicit configurations achieving $S_{2,n} = 6(n-1)$ for all $n \geq 2$, with separate constructions for even and odd n.

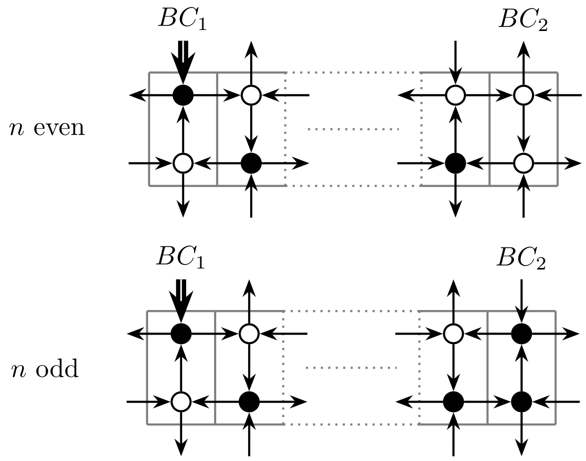

Figure 9 Configurations achieving $S_{2,n} = 6(n-1)$. The initial position of the ant is indicated by the double arrow. All intermediate columns have configuration $\begin{bmatrix} R \\ L \end{bmatrix}$. The ant starts with an initial motion within BC_1, traverses the intermediate columns to BC_2 where it bounces, returns to BC_1 for a second bounce, and finally reaches BC_2 again to perform an out motion.

4.3.2 Three-row Grids

When viewed column by column, a three-row grid (either vertical or horizontal) can be seen as an alternating succession of horizontal and vertical $G_{3,1}$ (see Figure 10).

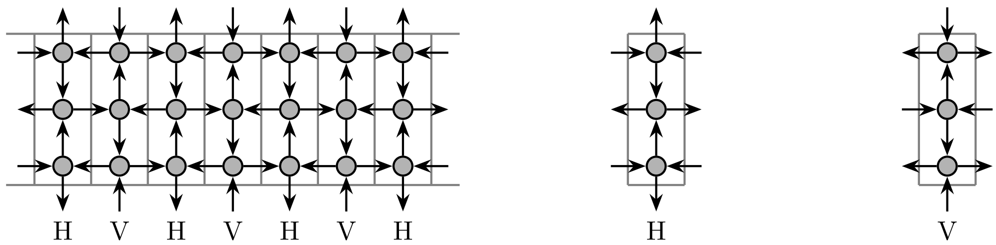

(a) Portion of three-row grid. **(b)** Horizontal $G_{3,1}$. **(c)** Vertical $G_{3,1}$.

Figure 10 Three-row grid viewed by columns.

The main result of this section is the following linear upper bound.

▶ **Theorem 8.** *For every integer $n \geq 2$, one has $S_{3,n} \leq 10n-4$.*

The proof of Theorem 8 relies on two ingredients: a blocking property of horizontal columns (Lemma 9) and a per-column step bound for vertical columns (Corollary 10).

▶ **Lemma 9.** *During the motion of the ant on a three-row grid, suppose the ant performs a crossing motion within a column that is a horizontal $G_{3,1}$ and subsequently re-enters it via an arc incident to a cell not exited during that crossing. Then the ant cannot perform any further crossing motion through this column before escaping the three-row grid.*

Proof. Let OC denote the horizontal $G_{3,1}$ under consideration (OC for Original Column). Assume without loss of generality that the ant crosses OC from left to right using cells of the top and the middle rows. The argument for other crossing types follows by symmetry. After the crossing, the ant can subsequently return to the column only from the right and in order to re-enter it through an arc incident to a cell different from the top and the middle cells, it must enter through an arc incident to a cell of the bottom row. An exhaustive case analysis on the color configuration of the bottom cell illustrated in Figure 11 shows that in all cases the ant escapes the three-row grid without performing any further crossing through OC.

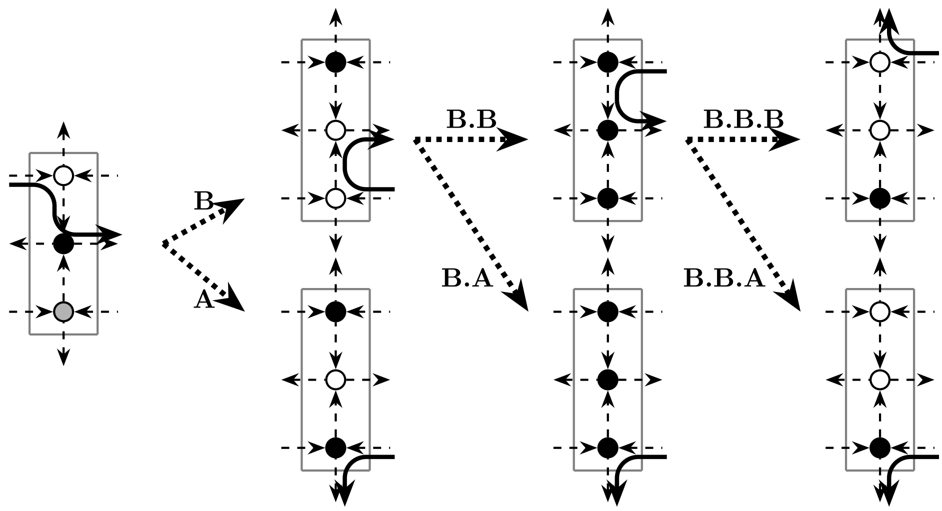

Figure 11 Exhaustive case analysis for the proof of Lemma 9. Curved solid arrows depict the motion of the ant. The initial crossing of OC uses the top and middle rows. Each sub-figure shows the color configuration of OC and the resulting motion. The labels A and B correspond to the two possible states of the bottom cell when the ant re-enters OC from the right: A when the bottom cell is in state L (black), and B when it is in state R (white). Subsequent labels ($B.A$, $B.B$, $B.B.A$, $B.B.B$) denote the corresponding branches of the case analysis.

◀

For simplicity, we say that a horizontal column is *blocking* if it is in a color configuration such that the ant cannot perform any further crossing motion through it before escaping the three-row grid. Using Lemma 9, we can bound the total number of steps performed within each vertical column depending on the type of its first motion.

There are three possible types of motion that the ant can perform on a column of a three-row grid which is a vertical $G_{3,1}$: Initial, Bouncing, Crossing motions.

▶ **Corollary 10.** *During its motion within a three-row grid, if the motion performed by the ant upon its first visit to a column that is a vertical $G_{3,1}$ is:*

1. *a crossing motion, then the ant performs at most six steps within this column before escaping the entire three-row grid. Moreover, these six steps consist of three crossing motions, two of which occur in the same direction;*

2. *a bouncing motion, then the ant performs at most ten steps within this column before escaping the entire three-row grid. Moreover, these ten steps consist of two bouncing motions within the same side and three crossing motions, two of which start from the side of the bouncing.*

We can now prove the main result.

Sketch of the Proof of Theorem 8. We decompose $S_{3,n} = SH_{3,n} + SV_{3,n}$, where $SH_{3,n}$ and $SV_{3,n}$ denote the maximum number of steps performed by the ant within horizontal and vertical columns, respectively. The key observation is that, apart from the initial step and the final escaping step (each occurring at most once), the motion of the ant can be decomposed into a succession of two-step segments within individual columns. Moreover, the dynamics alternates between horizontal and vertical columns: after visiting a horizontal column, the ant must move to a vertical one, and vice versa. Therefore, the total contribution of horizontal columns cannot exceed that of vertical columns by more than two steps, and we obtain $SH_{3,n} \leq SV_{3,n} + 2$.

It therefore suffices to bound the contribution of vertical columns. By Corollary 10, each non-boundary vertical column contributes at most 10 steps. The two boundary columns contribute strictly less, and a case analysis (depending on the parity of n) shows that $SV_{3,n} \leq 5n - 3$. Combining with $SH_{3,n} \leq SV_{3,n} + 2$, we obtain

$$S_{3,n} = SH_{3,n} + SV_{3,n} \leq (5n - 1) + (5n - 3) = 10n - 4. \qquad \blacktriangleleft$$

Lower bound for $S_{3,n}$

The upper bound is nearly tight. Explicit constructions (Figure 12) show that for every $n \geq 3$ $S_{3,n} \geq 10n - 12$ if n is even and $S_{3,n} \geq 10n - 13$ if n is odd. Moreover, our simulations for $n \leq 20$ yield exact escaping times consistent with these constructions.

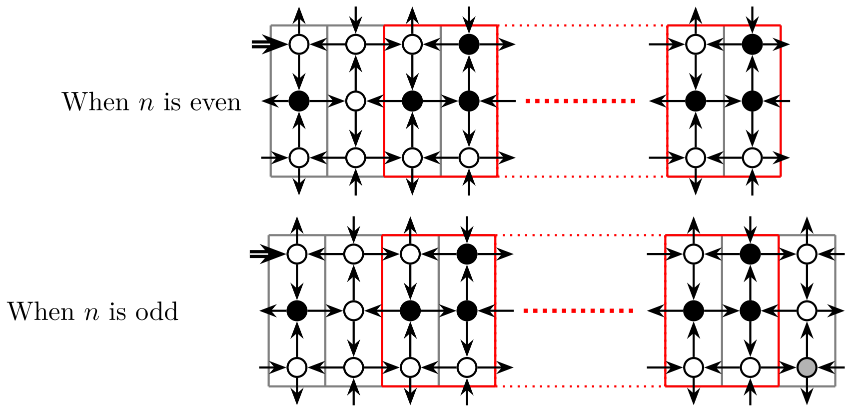

Figure 12 Configurations yielding lower bound for $S_{3,n}$. The initial position of the ant is indicated by the double arrow.

4.3.3 Four-row Grids: Lower bound and conjecture

Explicit constructions (Figure 13) show that for every $n \geq 14 : S_{4,n} \geq 34(n-5) + 20$. Moreover, our simulations indicate that $S_{4,n} = 34(n-5) + 20$ for even n with $14 \leq n \leq 18$ and odd n with $9 \leq n \leq 17$. These observations lead us to conjecture the following linear upper bound.

▶ **Conjecture 11.** *For every integer $n \geq 2$, one has $S_{4,n} \leq 34n$.*

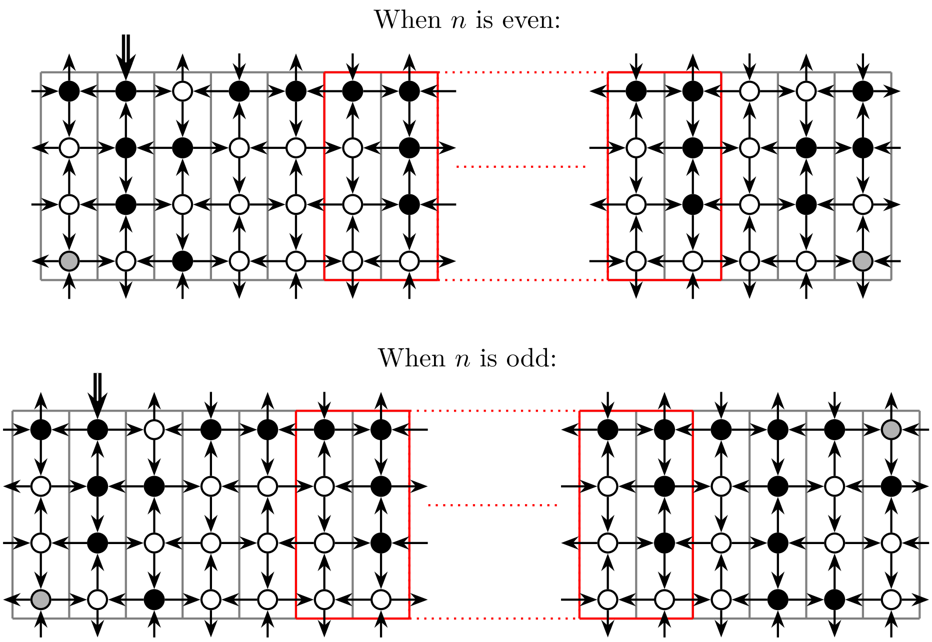

Figure 13 Configurations yielding lower bound for $S_{4,n}$. The initial position of the ant is indicated by the double arrow.

4.4 Upper Bound for the Escaping Time of Rectangular Domains

Using the same inductive decomposition as in Section 4.2, adapted to the rectangular setting, we now derive an upper bound for $S_{k,n}$ that improves on the general 2^{kn} bound for fixed k.

▶ **Theorem 12.** *For fixed $k \geq 2$ and $n \geq k$,*

$$S_{k,n} \leq \begin{cases} (6n-4) \cdot \left(\dfrac{n+1}{\sqrt{2}}\right)^{k-2} & \text{if } k \text{ is even,} \\ (10n-2) \cdot \left(\dfrac{n+1}{\sqrt{2}}\right)^{k-3} & \text{if } k \text{ is odd.} \end{cases}$$

In particular, $S_{k,n} \leq \left(\frac{n+1}{\sqrt{2}}\right)^k$.

Proof. We decompose $G_{k,n}$ as the union of the interior grid $G_{k-2,n}$ and two $G_{1,n}$, one along the top boundary and one along the bottom boundary (Figure 14).

By Remark 4, the ant starts from an in-boundary arc of $G_{k,n}$, reaches an in-boundary arc of $G_{k-2,n}$ in at most two steps, and then alternates between phases inside $G_{k-2,n}$ and bouncing phases on the two $G_{1,n}$, until it finally exits $G_{k,n}$ in at most two additional steps. If the ant returns to $G_{k-2,n}$ at most Y_n times after its initial entry, we obtain

$$S_{k,n} \leq (Y_n + 1) \cdot S_{k-2,n} + 2Y_n + 4.$$

It remains to bound Y_n. Since the decomposition involves only the top and bottom $G_{1,n}$ (two sides rather than four), the same per-row bouncing analysis as in Section 4.2 gives $Y_n \leq 2 \cdot \frac{n^2}{4} = \frac{n^2}{2}$. Substituting:

$$S_{k,n} \leq \left(\frac{n^2}{2} + 1\right) S_{k-2,n} + n^2 + 4.$$

From this inequality, by an induction on k, with base cases $S_{2,n} \leq 6(n-1)$ (for even k) and $S_{3,n} \leq 10n - 4$ (for odd k) given by Theorems 7 and 8 respectively, the result follows. ◀

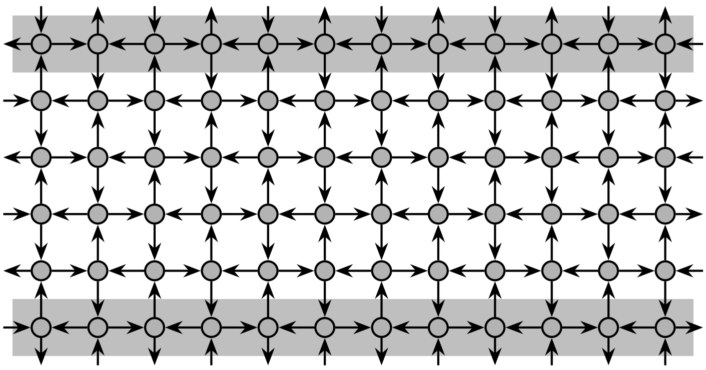

Figure 14 Decomposition of $G_{6,12}$ as the union of the interior grid $G_{4,12}$ (white region) and two $G_{1,12}$, one along the top boundary and one along the bottom boundary(gray shaded region).

5 Conclusion and Open Questions

We studied the escaping time of Langton's ant on finite connected domains of the square grid, establishing general structural properties and deriving upper bounds. We obtained a factorial upper bound for square domains and linear bounds for rectangular domains of height two and three, supported by exact values from simulations and matching or near-matching lower-bound constructions. More generally, for a fixed height k, we obtained an upper bound $\left(\frac{n+1}{\sqrt{2}}\right)^k$ for rectangular domains $G_{k,n}$. Several directions remain open.

Our simulation results for square domains ($n \leq 9$) suggest that $S_{n,n}$ grows significantly slower than the factorial upper bound $(n+1)!$, with values consistent with cubic growth $S_{n,n} \in O(n^3)$. Can the factorial bound be improved to a polynomial bound in n?

Extending the column-by-column analysis to grids of height four appears feasible, although the case analysis becomes significantly more complex. Preliminary simulations suggest a linear bound of the form $S_{4,n} \leq 34n$, and we have identified constructions achieving values close to this bound. Can this conjecture be proved?

More generally, while $\left(\frac{n+1}{\sqrt{2}}\right)^k$ guarantees a polynomial upper bound in n for every fixed k for $S_{k,n}$, the degree grows with k. Is there a function f such that $S_{k,n} \leq f(k)\,n$ for all $k \in \mathbb{N}$? In other words, is the escaping time linear in n for every fixed height k?

Computing exact values of $S_{k,n}$ for larger grids (e.g., 10×10 and beyond) could help refine these conjectures, and designing constructions yielding stronger lower bounds remains an important combinatorial challenge.

Finally, a better understanding of escaping time may contribute to clarifying the computational complexity of Langton's ant on finite grids, particularly for reachability problems.

References

1 Leonid A. Bunimovich. Many-dimensional lorentz cellular automata and turing machines. *International Journal of Bifurcation and Chaos*, 6(1):1127–1135, 1996.

2 Leonid A. Bunimovich and Serge E. Troubetzkoy. Recurrence properties of lorentz lattice gas cellular automata. *Journal of Statistical Physics*, 67:289–302, 1992.

3 Anahí Gajardo and Eric Goles. Dynamics of a class of ants on a one-dimensional lattice. *Theoretical Computer Science*, 322:267–283, 2004. `doi:10.1016/J.TCS.2004.03.012`.

4 Anahí Gajardo, Eric Goles, and Andrés Moreira. Generalized langton's ant: Dynamical behavior and complexity. In *STACS 2001*, volume 2010 of *LNCS*, pages 259–270. Springer, 2001. `doi:10.1007/3-540-44693-1_23`.

5 Anahí Gajardo, Victor H. Lutfalla, and Michaël Rao. Ants on the highway. *Natural Computing*, 24:497–509, 2025. `doi:10.1007/S11047-025-10018-9`.

6 Anahí Gajardo, Andrés Moreira, and Eric Goles. Complexity of langton's ant. *Discrete Applied Mathematics*, 117:41–50, 2002. `doi:10.1016/S0166-218X(00)00334-6`.

7 David Gale, Jim Propp, Scott Sutherland, and Serge E. Troubetzkoy. Further travels with my ant. *The Mathematical Intelligencer*, 17(3):48–56, 1995.

8 Patrick Grosfils, Jean Pierre Boon, E. G. D. Cohen, and Leonid A. Bunimovich. Propagation and organization in lattice random media. *Journal of Statistical Physics*, 97:575–608, 1999.

9 Takeo Hagiwara and Tatsuie Tsukiji. Hardness of approximation for langton's ant on a twisted torus. *Algorithms*, 13(12):344, 2020. `doi:10.3390/A13120344`.

10 Christopher G. Langton. Studying artificial life with cellular automata. *Physica D*, 22:120–149, 1986.

11 The OEIS Foundation Inc. Sequence a282425. `https://oeis.org/A282425`, 2017. On-Line Encyclopedia of Integer Sequences.

12 Serge Troubetzkoy. Lewis–parker lecture 1997: The ant. *Alabama Journal of Mathematics*, 21(2):3–13, 1997.

13 Tatsuie Tsukiji and Takeo Hagiwara. Recognizing the repeatable configurations of time-reversible generalized langton's ant is pspace-hard. *Algorithms*, 4:1–15, 2011. `doi:10.3390/A4010001`.